Published in final edited form as:
Cell. 2008 April 18; 133(2): 328–339. doi:10.1016/j.cell.2008.02.036.

CASK Functions as a Mg2+-independent neurexin kinase

Konark Mukherjee[1,2,*], **Manu Sharma**[1], **Henning Urlaub**[3], **Gleb P. Bourenkov**[5], **Reinhard Jahn**[2], **Thomas C. Südhof**[1,*], and **Markus C. Wahl**[4,*]

[1]Department of Neuroscience Howard Hughes Medical Institute University of Texas Southwestern Medical Center 6000 Harry Hines Blvd. Dallas, Texas 75390-9111, USA

[2]Department of Neurobiologie, Max-Planck-Institut für Biophysikalische Chemie Am Faßberg 11 D-37077 Göttingen, Germany

[3]Department of Bioanalytische Massenspektrometrie, and Max-Planck-Institut für Biophysikalische Chemie Am Faßberg 11 D-37077 Göttingen, Germany

[4]Department of Zelluläre Biochemie/Röntgenkristallographie Max-Planck-Institut für Biophysikalische Chemie Am Faßberg 11 D-37077 Göttingen, Germany

[5]MPG-ASMB AG Proteindynamik Deutsches Elektronen Synchrotron D-22603 Hamburg, Germany

Summary

CASK is a unique MAGUK protein that contains an N-terminal CaM-kinase domain besides the typical MAGUK domains. The CASK CaM-kinase domain is presumed to be a catalytically inactive pseudokinase because it lacks the canonical DFG-motif required for Mg^{2+}-binding. Here we show, however, that CASK functions as an active protein kinase even without Mg^{2+}. High-resolution crystal structures reveal that the CASK CaM-kinase domain adopts a constitutively active conformation that binds ATP and catalyzes phosphotransfer without Mg^{2+}. The CASK CaM-kinase domain phosphorylates itself and at least one physiological interactor, the synaptic protein neurexin-1, to which CASK is recruited via its PDZ-domain. Thus, our data indicate that CASK combines the scaffolding activity of MAGUKs with an unusual kinase activity that phosphorylates substrates which are recuited by the scaffolding activity. Moreover, our study suggests that besides CASK, other pseudokinases (10% of the kinome) could also be catalytically active.

Introduction

At least 1.7% of human genes encode protein kinases (Manning *et al.*, 2002). 10 % of all kinase domains have accumulated evolutionary changes that, according to our present understanding, render them catalytically inactive, prompting these to be designated “pseudokinases” (Manning *et al.*, 2002). Sequence analyses of these domains revealed evolutionarily conserved alterations in otherwise highly invariant motifs. For instance, the Ca^{2+}/calmodulin-dependent (CaM)-kinase domain of CASK (Ca^{2+}/calmodulin activated Ser-Thr kinase) is one of nine known pseudokinases that contain alterations in the canonical

*To whom correspondence should be addressed. TCS: Tel.: 214-648-1876; Fax: 214-648-1801;thomas.sudhof@utsouthwestern.edu. *KM: Tel.: 214-648-1903; Fax: 214-648-1801;konark.mukherjee@utsouthwestern.edu. *MCW: Tel.: ++49-551-201-1046; Fax: ++49-551-201-1197;mwahl@gwdg.de.

Supplementary Material Supplementary Materials include one table, thirteen figures, and Experimental Procedures for structural and mass-spectrometric studies.

Mg^{2+}-binding DFG (Asp-Phe-Gly) motif and are thought to have no catalytic activity (Boudeau *et al.*, 2006; Manning *et al.*, 2002).

CASK was simultaneously discovered in three different organisms: In biochemical experiments in vertebrates because of its binding to neurexins, which are synaptic cell-adhesion molecules (Hata *et al.*, 1996); in genetic experiments in *C. elegans* because it is encoded by the *Lin-2* gene that is essential for vulva development (Hoskins *et al.*, 1996); and by sequence analyses in *D. melanogaster* because CASK contains an N-terminal CaM-kinase domain (Martin and Ollo, 1996). Deletion or mutation of *CASK* leads to anomalous synaptic function and perinatal death in mice (Atasoy *et al.*, 2007), to severe developmental deficits in *C. elegans* (Hoskins *et al.*, 1996), or to behavioral and neurotransmitter-release abnormalities in *Drosophila* (Lopes *et al.*, 2001; Martin and Ollo, 1996; Zordan *et al.*, 2005). In humans, the *CASK* gene has been linked to X-linked optic atrophy and mental retardation in mapping and cohort studies (Dimitratos *et al.*, 1998; Froyen *et al.*, 2007). The evolutionary conservation of CASK and the severe deletion phenotypes suggest that CASK performs important biological roles, but the precise nature of its function has remained elusive.

CASK is composed of an N-terminal CaM-kinase domain that accounts for approximately half of its primary structure, and a C-terminal combination of domains that is typical of MAGUKs (membrane-associated guanylate kinases). The MAGUK-half of CASK includes an L27 domain, a PDZ domain (which was one of the first PDZ-domain structures determined (Daniels *et al.*, 1998)), an SH3-domain, and a C-terminal guanylate kinase domain that is thought to engage in inter- and intramolecular interactions (Hsueh *et al.*, 2000; Nix *et al.*, 2000).

Since the CASK CaM-kinase domain is presumed inactive, studies of CASK function have focused on its role as a MAGUK-type scaffolding protein. A large array of CASK interactions has been described: CASK associates stoichiometrically with Mint-1 (also called X11 or Lin-10) and Velis (also called MALS or Lin-7) that may be involved in organizing synapses (Borg *et al.*, 1998; Butz *et al.*, 1998). Consistent with a scaffolding activity, the CASK PDZ-domain binds to neurexins, syndecans, and SynCAMs, which are putative cell-adhesion molecules (Biederer *et al.*, 2002; Cohen *et al.*, 1998; Hata *et al.*, 1996; Hsueh *et al.*, 1998). CASK also associates with protein-4.1, and a trimeric complex composed of CASK, protein-4.1, and the cytoplasmic tail of neurexin-1 is a potent nucleator of actin polymerization (Biederer and Sudhof, 2001). CASK may recruit Ca^{2+} channels to the synapse (Maximov *et al.*, 1999), and target potassium channels (Leonoudakis *et al.*, 2004) and/or the Ca^{2+} pump 4b/Cl (Schuh *et al.*, 2003) to the plasma membrane. In *C. elegans*, the CASK homolog Lin-2 is implicated in proper localization of the EGF-receptor LET-23 (Hoskins *et al.*, 1996). CASK is proposed to bind PARKIN and function in its targeting and scaffolding at the synapse (Fallon *et al.*, 2002). Similarly, the CASK-Mint-1 complex has been implicated in targeting the NMDA-receptor subunit NR2B from Golgi to postsynapse via its interaction with dendritic kinesin KIF17 (Setou *et al.*, 2000). CASK also associates with CASKins (Olsen *et al.*, 2005) and liprins (Setou *et al.*, 2000), and might regulate transcription factors in the nucleus (Hsueh *et al.*, 2000). Moreover, CASK enhances Ether-a-go-go potassium currents via increasing its phosphorylation (Marble *et al.*, 2005). Finally, CASK may associate with CaM-kinase II (CaMKII), and modulate its phosphorylation state (Hodge *et al.*, 2006; Lu *et al.*, 2003; Zordan *et al.*, 2005). The regulation of phosphorylation was thought to be indirect in both the cases, as CASK was deemed a pseudokinase.

Here, we decribe high-resolution crystal structures of the CaM-kinase domain of CASK complexed to different nucleotides. These structures led us to hypothesize that despite the

lack of an appropriate Mg^{2+}-binding motif in its structure, CASK may nevertheless function as a protein kinase. Indeed, we show that unlike any known kinase, the CASK CaM-kinase domain catalyzes autophosphorylation and phosphotransfer to the cytoplasmic tail of neurexin-1 in the absence of Mg^{2+}. Our data suggest that CASK is unique among protein-kinases in that its CaM-kinase domain uses an unusual mechanism to phosphorylate substrates which are recruited via its MAGUK component.

Results

The CASK CaM-kinase domain adopts a constitutively active conformation

We compared the sequences of the CASK CaM-kinase domain with the homologous kinases CaMKI (≈ 37 % identity) and CaMKII (≈ 44 % identity; Suppl. Fig. S1). Based on the sequence homology, we produced a recombinant CASK CaM-kinase domain (residues 1-337; note that these residues are identical in mouse, rat and human CASK), and determined its crystal structure. The purified protein was crystallized in two space groups, a reticularly twinned triclinic form (P1 form) and an orthorhombic form ($P2_12_12_1$ form). The structures of both forms were solved by molecular replacement using the coordinates of the CaMKI kinase domain (Goldberg *et al.*, 1996) (PDB ID: 1A06), and refined at 2.2 Å (P1 form) and 1.85 Å ($P2_12_12_1$ form) resolution (Fig. 1, Suppl. Fig. S3, and Suppl. Table S1). The structures of the CASK CaM-kinase domain in the two crystal forms are highly similar (pairwise Cα root-mean-square deviation ≈ 0.4 Å), indicating that the overall structure of the domain was not significantly influenced by the crystalline environment (Figs. 1A,B, Suppl. Figs. S2A and S3). Both the P1 and $P2_12_12_1$ structures exhibited uninterrupted backbone electron densities throughout the entire domain from residues 5 to 304.

The catalytic core of protein kinases can be divided into an N-terminal lobe that is involved in ATP binding, and a C-terminal lobe that binds and positions the substrate in addition to contributing to ATP binding and ATP activation (Taylor *et al.*, 2004). In the active state conformation, protein kinases adopt a very similar overall fold that positions the elements in the N- and C-terminal lobes involved in substrate binding and catalysis in a canonical fashion (Huse and Kuriyan, 2002; Nolen *et al.*, 2004). In the inactive state, in contrast, protein kinases adopt different overall folds.

The CASK CaM-kinase domain exhibits a typical protein kinase fold with an N-terminal lobe dominated by a five-stranded β-sheet and an α-helical C-terminal lobe (Figs. 1A,B, and Suppl. Figs. S2 and S3). Comparison of the CASK CaM-kinase domain structures with those of other protein kinases revealed that the relative orientation of N- and C-terminal lobes in the CASK CaM-kinase domain is very similar to that of the active state of the death-associated protein kinase 1 (DAPK1) in a complex with the ATP analog AMPPNP (Tereshko *et al.*, 2001) (PDB ID: 1IG1), resembling the catalytically active “closed conformation” (Figs. 1A,B, and D, and Suppl. Fig. S2C). In contrast, the inactive form of CaMKI adopts a distinct “open conformation” with respect to the two lobes, resulting in a diminished affinity for nucleotides (Figs. 1C and Suppl. Fig. S2B) (Goldberg *et al.*, 1996), that is very different from that of the CASK CaM-kinase domain.

Specific structural elements of the CASK CaM-kinase domain

Equivalents of all the essential elements were found in this domain (Figs. 1A,B, and Suppl. Figs. S2 and S3). The N-terminal lobe encompasses a Gly-rich loop (residues 19–24 in CASK; brown) and a Lys-Glu ion pair (Lys41 and Glu62 in CASK) (Suppl. Fig. S5C). Furthermore, it displays an activation segment (green) and a catalytic loop (residues 141–146 in CASK; yellow). This catalytic loop is positioned normally in CASK CaM-kinase domain, although the invariant Asn146 is substituted by Cys (Suppl. Fig. S1). In protein

kinases, Asn146 in the catalytic loop coordinates Mg^{2+} and stabilizes the catalytic loop by forming a hydrogen bond with the catalytic Asp141. In the absence of an Asn at position 146, the catalytic Asp141 of the CASK CaM-kinase domain engages in a number of alternative interactions, which stabilize its conformation and the catalytic loop. Notably, the smaller Cys146 side chain is still able to engage in a hydrogen bond with the backbone carbonyl of Asp141 (Suppl. Fig. S5A,B).

In kinase structures corresponding to an inactive state, such as the structures of CaMKI, MnK1 and MnK2, the activation segment is often displaced from its binding site in the C-terminal lobe, and frequently is disordered (Fig. 1C and Suppl. Fig. S2B) (Goldberg *et al.*, 1996; Jauch *et al.*, 2006; Jauch *et al.*, 2005). However, in the CASK CaM-kinase domain, the activation segment is fully ordered, and its C-terminal portion is cradled in an active state conformation within the C-terminal lobe. Superimposing CDK2 in complex with cyclin A, a substrate peptide and ATP (PDB ID 1QMZ) with the CASK structure suggests that substrate peptides can bind on top of the activation segment of the CASK CaM-kinase domain along the mouth of the nucleotide binding cleft. ATP thus could be bound next to the substrate into the nucleotide binding pocket with its γ-phosphate pointing towards the substrate peptide, in a fully active orientation (Suppl. Fig S4B).

The C-terminal lobe of the CASK CaM-kinase domain contains an equivalent of the Mg^{2+}-binding loop, but the DFG-motif within the loop is altered to GFG by the Asp162Gly substitution. This loop is ordered in the CASK CaM-kinase domain structure (orange) as in DAPK1, while it is partially disordered in the CaMKI structure (Fig. 1C and S2B). Overall, the potential catalytic elements of the CASK CaM-kinase domain could be superimposed onto corresponding elements in the DAPK1-AMPPNP co-crystal structure (Suppl. Fig. S2C), confirming that the structures exhibit core features and functional elements closely resembling an inherently active-state fold; dissimilar to the inactive CaMKI fold.

The nucleotide binding pocket of the CASK domain was occupied by 3'-AMP in the crystal structure (Figs. 1A and 2D, and Suppl. Figs. S2A and S3, and Suppl. Table S1). The bound 3'-AMP is likely a byproduct of bacterial RNA degradation during protein purification. Upon soaking the crystals in 5'-AMPPNP in the presence of equimolar Mg^{2+}, the 3'-AMP could be displaced by 5'-AMPPNP, suggesting a readily accessible adenine-nucleotide binding site (Figs. 1B, 2B, and 2E, and Suppl. Fig. S2A). The CASK CaM-kinase domain, thus, adopts an intrinsically active conformation amenable to nucleotide binding.

To better characterize the mode of nucleotide binding to the CASK CaM-kinase domain, we solved the structure of the best derivative crystals containing 5'-AMPPNP at 2.3 Å resolution (P1 form; Suppl. Table S1). The binding mode of the nucleotide in the pocket is reminiscent of the AMPPNP-bound DAPK1 structure (Tereshko *et al.*, 2001). The N1 and N6 amino groups of the adenine form hydrogen-bonds with the backbone NH of Met94 and the oxygen of Glu92, respectively. Similar to the orientation of AMPPNP in the DAPK1 structure, the adenine base of the 5'-AMP moiety was found in an *anti* conformation, and the sugar retained a C2'-*endo* conformation (Fig. 2B). The overall binding and orientation of the 5'-AMP portion of the nucleotide is in agreement with the binding of ATP to generic protein kinases in an active conformation (Figs. 2A–2E).

In active protein kinases, bound nucleotides are coordinated by a Mg^{2+} ion and by amino acid residues in the surrounding pocket. DAPK1 coordinates the α-phosphate of AMPPNP through a hydrogen bond with Lys42. In addition, a Mg^{2+} ion (that in turn is bound to the Asp of the DFG-motif and Asn of the catalytic loop) bridges the α- and β-phosphates (Tereshko *et al.*, 2001) (Fig. 2C). In the CASK CaM-kinase structure containing AMPPNP, the α-phosphate was resolved and found to be positioned between the side chains of His145

and Lys41, without directly contacting either residue. Rather, the α-phosphate is heavily hydrated and maintains water-mediated contacts to various sites in the pocket (Fig. 2B and Suppl. Fig. S5C). The β- and γ-phosphates, in contrast, were disordered; no Mg^{2+} ion could be discerned in the pocket, despite its presence in the crystallizing milieu. With the lack of a canonical Mg^{2+} binding motif in the CASK CaM-kinase domain, the phosphates may be de-coordinated by the coupled Mg^{2+}.

Thus, the structural data suggest that the CASK CaM-kinase domain is capable of coordinating ATP in a canonical orientation without Mg^{2+}, and is equipped with all the structural components of a catalytic kinase, with noticeable substitutions in both the Mg^{2+}-coordinating residues (Asp162Gly and Asn146Cys) and a consequential de-coordination of the β- and γ-phosphates of ATP. These results indicate that the CASK CaM-kinase domain may physiologically bind nucleotides without Mg^{2+}-binding. To explore this hypothesis, we first studied nucleotide binding to the CASK CaM-kinase domain.

ATP binds to the CASK CaM-kinase domain in a Mg^{2+}-sensitive manner

Since the crystal structure showed that the CASK CaM-kinase domain binds ATP, we tested whether the domain interacts with the ATP analog TNP-ATP, that becomes fluorescent when inserted into the hydrophobic ATP-binding pocket (Stewart *et al.*, 1998).

In the presence of EDTA, the CASK CaM-kinase domain induced a 3 to 5-fold increase in fluorescence intensity, and a blue-shift of the emission maximum, of TNP-ATP (Fig. 3A). ATP partly blocked this fluorescence increase. Titrations revealed that a 500-fold excess of ATP reduced the TNP-ATP fluorescence by 50% ($K_i^{ATP} \approx 0.365$ mM), consistent with competitive binding of ATP and TNP-ATP to the same site, that exhibits a much higher affinity for TNP-ATP than for ATP (Stewart *et al.*, 1998). Even a 1,000-fold excess of GTP had no effect on TNP-ATP binding, pointing to adenine nucleotide-specificity of the pocket (Fig. 3B). To further dissect the specificity of nucleotide binding to the CASK CaM-kinase domain, we examined the inhibition of TNP-ATP binding by adenine, ATP, ADP, 5'-AMP, 3'-AMP, and cAMP. Only ATP inhibited TNP-ATP binding to the CASK CaM-kinase domain efficiently, while all other naturally occurring nucleotides tested had little effect (Fig. 3C), suggesting that the CASK CaM-kinase domain specifically binds ATP.

Although certain kinases can utilize Mn^{2+} for enzymatic activity *in vitro* (Nirmala *et al.*, 2006), Mg^{2+} is the only divalent ion available at optimal concentration *in vivo*. Thus, kinases have evolved to exclusively utilize Mg^{2+} as a cofactor for catalysis (Waas *et al.*, 2004). We tested the effect of divalent cations on TNP-ATP binding to the CASK CaM-kinase domain. Surprisingly, addition of Mg^{2+} inhibited the increase in TNP-ATP fluorescence induced by the CASK CaM-kinase domain (Fig. 3A). Titration experiments demonstrated that the TNP-ATP – CASK CaM-kinase domain complex is diminished at higher than equimolar concentrations of Mg^{2+} ($K_iMg^{2+} \approx 10.41$ μM), suggesting that Mg^{2+} competitively inhibits ATP-binding to the CASK CaM-kinase domain (Suppl. Fig. S6B). Mn^{2+} and Ca^{2+} could also inhibit TNP-ATP binding (Fig. 3D). The TNP moiety of TNP-ATP could potentially form atypical contacts in the binding site, as demonstrated for the histidine kinase CheA (Bilwes *et al.*, 2001), and TNP-ATP binding may not be representative of ATP binding. To address this possibility, we tested binding of the CASK CaM-kinase domain to γ^{32}P-ATP using a dot-blot assay (Suppl. Fig. S6A). This assay revealed that Mg^{2+} significantly inhibited binding of γ^{32}P-ATP to the CASK CaM-kinase domain. Hence, ATP binding to the CASK CaM-kinase domain is disrupted by biologically abundant divalent cations, including Mg^{2+}, consistent with the absence of a DFG-motif and a C-loop Asn in its structure.

CASK CaM-kinase domain is an active kinase

Coordination of the β- and γ-phosphates of ATP by Mg^{2+}-ions catalyzes phosphotransfer reactions by protein kinases (Adams, 2001; Hanks and Hunter, 1995). The fact that Mg^{2+}, if anything, impairs ATP binding by the CASK CaM-kinase domain is consistent with the notion that this domain is indeed a `pseudokinase'; despite its constitutively active conformation and avid ATP binding. To test this, we examined whether the CASK CaM-kinase domain exhibits autophosphorylation activity, which is typical for CaM-kinases and can be employed as a test for kinase activity (Hanley *et al.*, 1988).

Strikingly, the CASK CaM-kinase domain was autophosphorylated with nearly 13 % efficiency (Fig. 4A). Autophosphorylation was independent of Mg^{2+}, since it was carried out in Mg^{2+}-free buffer containing 2 mM EDTA. Tandem mass-spectrometry identified a single autophosphorylated CASK peptide containing residues 141–159 (DVKPHCVLLAS<u>K</u>ENS<u>A</u>PVK; data not shown). The phosphorylated peptide is located in a surface-exposed loop preceding the GFG motif (Suppl. Fig. S4A). Since it is remote from the substrate binding pocket, we speculate that autophosphorylation occurs in *trans*.

The autophosphorylation assay was used to calculate the Michaelis constant of the CASK CaM-kinase domain for ATP (K_m^{ATP}) (Fig. 4B), revealing a K_m^{ATP} of ≈ 0.563 mM, which is within the range of K_m^{ATP} for active kinases (Warmuth *et al.*, 2007). We measured the limiting rate of autophosphorylation in experiments that approached saturation. Again, the V_{max} for autophosphorylation of the CASK CaM-kinase domain (≈ 4.9 nmol/μmol enzyme/min), although low, is similar that of some other kinases, such as *Giardia lamblia* PKA (V_{max} ≈ 6.2 nmol/μmol enzyme/min) (Abel *et al.*, 2001).

Mg^{2+} and other divalent cations inhibited but did not abolish the auto-phosphorylation of CASK, presumably by reducing its ATP affinity (Fig. 4C). Inhibition by superstoichiometric Mg^{2+} suggests that the CASK CaM-kinase domain is optimally active in the presence of unchelated free ATP, and that the cellular Mg^{2+} content may regulate the kinase activity of CASK *in vivo* by limiting the free-ATP levels in the cytosol. To examine whether catalytic phosphotransfer can occur near neuronal levels of free Mg^{2+} (0.3–0.5 mM; (Brocard *et al.*, 1993; Taylor *et al.*, 1991)), we measured the autophosphorylation of the CASK CaM-kinase domain as a function of incrementally increased Mg^{2+}-concentrations. We found that Mg^{2+} steeply inhibited the CaM-kinase domain autophosphorylation at low concentrations, but that the inhibition saturated at higher Mg^{2+}-concentrations, such that a significant amount of residual autophosphorylation (>33% of maximum) remained even at high Mg^{2+} concentrations (Fig. 4D). The inhibition constant for Mg^{2+}-dependent inhibition of phosphotransfer ($K_i^{Mg^{2+}}$ ≈ 61 μM; Fig. 4D) parallels that of the Mg^{2+}-dependent inhibition of ATP binding ($K_i^{Mg^{2+}}$ ≈ 10.41 μM; Suppl. Fig. S6B), suggesting that the inhibition of phosphotransfer by Mg^{2+} is a result of the Mg^{2+}-dependent disruption of ATP-coordination. These data indicate that the concentration of ATP-Mg^{2+} in the neuronal cytoplasm should allow physiological catalysis by CASK, but this catalytic activity of CASK may be regulated by changes in the cytosolic divalent ion concentration.

CASK phosphorylates neurexin-1 *in vitro* and *in vivo*

CASK is abundant in brain (Hata *et al.*, 1996), and may associate with the pre-synaptic active zone (Olsen *et al.*, 2006),. Since brain contains relatively high concentrations of free ATP (Foskett *et al.*, 2007; Mak *et al.*, 1999; Rubin and Brown, 1988; Taylor *et al.*, 1991) and relatively low concentrations of free Mg^{2+} (Brocard *et al.*, 1993; Gotoh *et al.*, 1999; Kato *et al.*, 1998), the Mg^{2+}-dependent inhibition of the CASK CaM-kinase domain does not eliminate the possibility that this domain functions as a kinase. To test this, we examined

the effect of CASK kinase activity on neurexin-1β (neurexin-1), a CASK-interactor at the synapses (Hata *et al.*, 1996).

We first investigated the phosphorylation of the cytoplasmic C-terminal tail of neurexin-1 by the isolated CASK CaM-kinase domain (that is, the domain without the associated MAGUK domains) *in vitro*. Phosphorylation assays revealed that the CaM-kinase domain directly phosphorylates the neurexin-1 C-tail, and that this activity is strongly inhibited by Mg^{2+} (Suppl. Fig. S7). However, the phosphotransfer was minimal, and no phosphorylated peptide was detectable by mass spectrometry (data not shown).

Full-length CASK binds to neurexins via its PDZ-domain, and CASK co-localizes and co-precipitates with neurexins (Suppl. Fig. S8A,B and S9 (Hata *et al.*, 1996)), suggesting that the interaction of CASK with neurexins via the PDZ domain may facilitate phosphotransfer. To test this hypothesis, we measured phosphotransfer to the neurexin-1 cytoplasmic tail in a complex with full-length CASK. Indeed, we found that neurexin-1 was efficiently phosphorylated (Fig. 5A). These experiments, performed with a vast excess of neurexin, nevertheless resulted in a phorphorylation stoichiometry of ≈ 17 %. Whereas, CASK autophosphorylation was undetectable in these reactions, possibly due to competition with a substrate. The net rate of phosphotransfer to neurexin-1 (V_{max} ≈ 159.4 nmol/μmol enzyme/min) was 30-fold faster than the rate of CASK autophosphorylation, suggesting that neurexin, when complexed to CASK, is a substrate for the CaM-kinase domain (Figs. 5A,B). The K_m^{ATP} of neurexin-1 phosphorylation by CASK (≈ 748.7 μM) was similar to that of autophosphorylation reactions, consistent with the notion that ATP utilization by CASK is not enhanced by the co-localization and availability of an optimal substrate (Fig. 5B). Improved efficiency of phosphotransfer to the CASK-associated neurexin-1 thus could be attributed to increased local substrate concentration mediated by the PDZ domain-mediated interaction. The high phosphorylation efficiency in CASK-neurexin-1 complexes allowed phosphopeptide mapping of the neurexin-1 C-tail by LC-MS-MS. Peptides comprising residues 422 to 433 of neurexin-1 (QPSSAKSANKNK) were detected with single and double-phosphates, establishing that the neurexin-1 C-tail is directly phosphorylated by CASK (not shown).

In CASK, the L27 domain links the CaM-kinase domain to the PDZ domain, but deletion of this linker region ($CASK^{-linker}$) had no effect on neurexin phosphorylation (Suppl. Fig. S10). This result indicates that the L27 domain is not directly involved in CASK-mediated phosphorylation, although binding of Velis to this domain (Butz *et al.*, 1998) may inhibit phosphorylation of a substrate bound to the PDZ-domain, an exciting possibility that would provide for additional regulation of CASK activity.

We next examined whether CASK can phosphorylate neurexin-1β under physiological conditions. Co-expression of a CASK-EGFP fusion protein with a neurexin-1β cherry fusion protein recruits CASK from the cytosol to the plasma membrane, and increases phosphorylation of neurexin-1β (Suppl. Fig. S8A,C). However, in these experiments we detected significant phosphorylation of neurexin-1β in the absence of CASK, suggesting that not surprisingly, other kinases also phosphorylate neurexin-1β.

Neurexin phosphorylation by CASK is regulated by neuronal-activity

We explored neurexin phosphorylation within a neuronal context in rat primary hippocampal cultures. Since β-neurexins are far more prevalent in these cultures, we decided to use these as our readout. Phosphorylated β-neurexins could be detected in mature neurons at 14 days *in vitro* (DIV) (Fig. 6A).

Cytosolic Mg^{2+} and Ca^{2+} concentrations are increased by synaptic activity (Brocard *et al.*, 1993; Gotoh *et al.*, 1999; Kato *et al.*, 1998). β-neurexin phosphorylation increased dramatically (more than 2-fold) when synaptic activity-driven divalent ion fluxes were suppressed (with APV, a NMDA-receptor antagonist and TTX, a Na^{+}-channel blocker) (Fig. 6A). These drugs had no effect on β-neurexin phosphorylation prior to the development of mature synapses (at 6 DIV) (data not shown). Since CASK, contrary to other kinases (Fig. 6A), is inhibited by divalent ions, enhanced neurexin phosphorylation upon synaptic inactivation is strongly suggestive of CASK kinase activity.

To test whether CASK is directly responsible for β-neurexin phosphorylation in neurons, we used a knockin-knockout approach. Primary hippocampal cultures from CASK knock-in mice, containing Lox-P sites flanking the *CASK* gene, were transduced with GFP-Cre recombinase fusion protein, using a lentiviral vector system (Atasoy *et al.*, 2007). Compared to the neurons from littermate wild type mice (WT), β-neurexin phosphorylation was reduced by nearly 40 % in CASK-knockout (CASK KO) neurons (Fig. 6B).

Since CASK has been proposed to act as an adaptor for various molecules, including other kinases (Kaech *et al.*, 1998; Lu *et al.*, 2003), disrupted docking of another kinase in the CASK KO neurons could have resulted in the reduced phosphorylation of β-neurexins. To preserve the adaptor function of CASK, a dominant-negative approach was used – that specifically targeted the kinase activity of CASK CaM-kinase domain. We developed a catalytically impaired CASK-mutant that could act as a dominant-negative competitor, when introduced into a neuron. Most studies involving the inactivation of classical protein kinases target residues thought to be involved in either γ-phosphate or substrate positioning (for instance Asp of HRD motif). Since the γ-phosphate of ATP bound to CASK CaM-kinase domain is already disordered, likely due to the lack of Mg^{2+}-coordinating Asp of DFG motif, such a strategy may be ineffectual (Supp Fig. S13). Thus, based on the stereochemistry of ATP-coordination within the nucleotide-binding pocket of CASK (Fig. 2B), we mutated Ser24 and Val26 to Asp and Leu, respectively (S24D, V26L). The CaM-kinase domain of CASK bearing this double mutation (referred to as $CASK^{SV}$) behaved as a hypomorph *in vitro*, evident from the dramatic reduction in both, autophosphorylation (Suppl. Fig. S11A) as well as neurexin C-tail phosphorylation (Suppl. Fig. S11B). Importantly, $CASK^{SV}$ retained the ability to bind ATP (data not shown), suggesting that it adopts the active conformation, and presumably retains native molecular interactions. In particular, $CASK^{SV}$ still binds efficiently to neurexin-1 via its PDZ-domain (data not shown), thus acting as a dominant-negative competitor of the wild type kinase.

We transfected rat hippocampal neurons at high efficiency with wild-type CASK ($CASK^{wt}$)or the $CASK^{SV}$ variant, as EGFP-fusion proteins (Fig. 6C). Expression of $CASK^{wt}$ produced an almost 2-fold increase in β-neurexin phosphorylation, whereas the expression of $CASK^{SV}$ caused an almost 2-fold decrease in β-neurexin phosphorylation (Fig. 6C). Since the expression of $CASK^{wt}$ and the kinase-hypomorph $CASK^{SV}$ assert diametrically opposite effects on the β-neurexin phosphorylation-state, this phosphotransfer is likely a direct consequence of CASK kinase activity. Together, these results demonstrate that CASK physiologically phosphorylates endogenous neurexins in neurons, and this phosphorylation is regulated by the synaptic acitivity-driven fluxes of divalent ions.

Discussion

In this study, we describe the crystal structure and biochemical properties of the CaM-kinase domain of CASK. We demonstrate that CASK functions as an active protein kinase that phosphorylates neurexins – and presumably other target proteins – by an unusual and novel mechanism. These observations are not only important for our understanding of CASK, an

enigmatic yet essential MAGUK protein with a CaM-kinase domain that is completely conserved in vertebrates, but also for our concept of "pseudokinases" in the kinome, which may turn out to be enzymatically active kinases with special properties.

Mg^{2+}-independent activity of CASK CaM-kinase domain

Mg^{2+} acts as an obligate cofactor for ATP-binding and phosphotransfer in all known kinases (Adams, 2001; Waas *et al.*, 2004). Here, we demonstrate that the CASK CaM-kinase domain is a physiologically active kinase that catalyzes phosphotransfer from ATP to proteins even in the complete absence of Mg^{2+}. To our knowledge, CASK is the first kinase, indeed the first nucleotidase, known to perform catalytic phosphotransfer in the absence of Mg^{2+}.

The structure of the CASK CaM-kinase domain determined here, and comparison of its structure with those of other kinases, illustrates that the CaM-kinase domain of CASK adopts a constitutively active conformation (Figs. 1 and 2, and Supp. Figs. S2 and S3). Biochemical and enzymatic assays demonstrated that CASK binds ATP independent of Mg^{2+}, and catalyzes autophosphorylation and neurexin-1 phosphorylation in the absence of Mg^{2+} (Figs. 3, 4 and 5). Compared to other kinases, CASK contains non-canonical residues at several conserved positions of the nucleotide-binding pocket, which may account for its unusual catalytic mechanism. Both of the classical metal-coordinating residues are substituted (Asn146Cys and Asp162Gly; see Supp. Fig. S1). Moreover, Glu143 of the catalytic-loop directly coordinates the metal ion in DAPK1; while in CASK, this Glu is altered to His (Glu145His), which might repel Mg^{2+} electrostatically. These changes likely contribute to the absence of Mg^{2+} coordination in the CASK CaM-kinase domain, resulting in the de-coordination of β- and γ-phosphates of ATP in the presence of Mg^{2+}. However, in the nucleotide binding pocket of CaMKII, the adenine base of ATP makes the most important contacts for the positioning of nucleotide (Kwiatkowski and King, 1987). A similar observation was made for the binding of 3'-AMP in one of our CASK CaM-kinase structures (Supp. Fig. S3). Thus, an altered Mg^{2+}-coordinating sequence does not exclude ATP-binding and, as shown here, does not exclude catalysis. Importantly, similar to the CASK CaM-kinase domain, other "pseudokinase" domains with non-canonical Mg^{2+}-binding motifs may coordinate ATP and phosphorylate physiological substrates as well.

Constitutively active CASK kinase is regulated by substrate recruitment

CASK is also unusual compared to any other member of the CaM-kinase family in that its CaM-kinase domain exhibits a constitutively active conformation (Supp. Fig. S2). In an archetypal CaM-dependent kinase, the catalytic domain is followed by an autoinhibitory domain that constitutively inhibits kinase activity, but is disinhibited by Ca^{2+}/calmodulin binding (Goldberg *et al.*, 1996). Indeed, the CASK CaM-kinase domain is followed by a sequence that is homologous to the autoinhibitory domain of CaM-kinases (Supp. Fig. S1), which also binds Ca^{2+}/calmodulin (Hata *et al.*, 1996). However, unlike typical CaM-kinases, the autoinhibitory helix (αR1) of CASK does not engage in direct contacts with the ATP-binding cleft (Fig. 1 and Supp. Fig. S3). We also did not discern evidence for further C-terminal residues interacting with the ATP binding cleft, as in CaMKI, and we detected no stimulatory effect of Ca^{2+} and/or calmodulin on the CASK kinase activity (data not shown). In CaM-kinases, the autoinhibitory domain acts by competition with the substrate. The pseudosubstrate region of the CASK sequence that is homologous to the autoinhibitory domain contains Arg288Leu and Gln289Pro substitutions that result in a sub-optimal pseudosubstrate helix (Supp. Fig. S1; (Smith *et al.*, 1992)) and is missing part of the consensus substrate motif (RXXT/S). Thus, the CASK CaM-kinase domain appears to retain a non-functional autoinhibitory domain as an evolutionary vestige of CaM-kinases. CASK, therefore, differs from other, evolutionarily closely related CaM-kinase domains not only in

its Mg^{2+}-independence, but also in its inherently "closed" active conformation which binds to nucleotides constitutively.

An almost essential consequence of the constitutively active conformation of the CASK CaM-kinase domain is that the domain exhibits a very low catalytic rate, as shown in autophosphorylation measurements (Fig. 4) and in measurements of neurexin-1 phosphorylation by the isolated CaM-kinase domain of CASK lacking its neurexin-binding PDZ-domain (Suppl. Fig. S7). Mechanistically, this low rate is likely due to the loss of Mg^{2+}-coordination by the domain. The low catalytic rate of the CASK CaM-kinase domain presumably serves to ensure that the kinase does not phosphorylate potential substrates randomly. We show that the phosphorylation rate of neurexin-1 is increased dramatically, however, when full-length CASK forms a complex with neurexin-1 via the PDZ-domain of CASK (Fig. 5). The binding of neurexin-1 to CASK probably increases the phosphotransfer efficiency by increasing the substrate specificity and the local substrate concentration. This result suggests a general mechanism for CASK kinase activity, whereby CASK couples an intrinsically slow but constitutively active kinase domain to a PDZ-domain that recruits the substrates to the kinase domain, thereby increasing the local substrate concentration by several orders of magnitude (see model in Fig. 7). According to this model, CASK unites two separate functions – the recruitment activity of MAGUKs and the kinase activity of the CaM-kinase domain – into a single unit whose objective is phosphorylation of specific interacting proteins (Fig. 7).

Physiological implications

CASK phosphorylates neurexin-1 *in vitro* and *in vivo* in a reaction that depends on a catalytically active CaM-kinase domain (Fig. 5 and 6). β-neurexins, described here as a substrate of CASK, is a pre-synaptic cell-adhesion molecule ((Nam and Chen, 2005; Ushkaryov *et al.*, 1992); reviewed in (Missler *et al.*, 2003)). Its heterotypic binding to the post-synaptic neuroligins may be involved in synaptic function (Missler *et al.*, 2003), and could induce synapse formation even on non-neuronal co-cultured cells (Graf *et al.*, 2004). The neurexin-neuroligin interaction is a candidate for synaptic specialization and pre-post synapse communication (reviewed in (Cline, 2005; Lise and El-Husseini, 2006; Yamagata *et al.*, 2003)). Both neurexin (via linkage and copy number analyses) and neuroligin mutations have been linked to autism spectrum disorders in human cohort studies (Jamain *et al.*, 2003; Szatmari *et al.*, 2007). Deletion of CASK may be connected to X-linked optic atrophy and mental retardation, according to human mapping and cohort studies (Dimitratos *et al.*, 1998; Froyen *et al.*, 2007). The evolutionary conservation of CASK and neurexins, and their central importance for survival and synaptic function in mice (Atasoy *et al.*, 2007; Missler *et al.*, 2003) indicates that neurexin phosphorylation by CASK may be crucial to neuronal function.

In addition to the control of CASK kinase activity by the PDZ-domain mediated substrate recruitment, we examined whether it is regulated by synaptic activity-driven rise in Ca^{2+} and Mg^{2+} levels (Brocard *et al.*, 1993; Gotoh *et al.*, 1999; Kato *et al.*, 1998). In neurons, application of glycine with glutamate augments the free-Mg^{2+} level from a resting 0.5 mM up to 11 mM – a 22-fold increase (Brocard *et al.*, 1993); in addition to the activity-driven Ca^{2+} influx. Cytosolic free-ATP levels, and thus the CASK kinase activity, could be regulated by these changes in divalent ions (Kargacin and Kargacin, 1997). Only in synaptically active mature neurons, we observed a strong increase in neurexin phosphorylation upon silencing synapses, indicating that contrary to other kinases, CASK kinase is inhibited by neuronal activity (Fig. 6A). We envision that CASK kinase activity is maximal during neuronal development and synaptogenesis, and declines with the onset of synaptic function, but is reactivated when neurons are silent. This developmentally regulated

activity is in line with the phenotypic defects in CASK knockout mice (Atasoy *et al.*, 2007) as well as the developmental nature of CASK- and neurexin-related pathologies (Froyen *et al.*, 2007; Szatmari *et al.*, 2007).

Moreover, CASK is expressed ubiquitously at low levels (Hata *et al.*, 1996). The non-neuronal functions of CASK are evident from developmental defects in CASK/Lin-2-null animals, such as cleft palate in mice (Atasoy *et al.*, 2007) and vulval dysgenesis in *C. elegans* (Hoskins *et al.*, 1996). The rescue experiments in *C.elegans* revealed that point mutants of the CASK CaM-kinase domain were significantly less capable of rescuing the Lin-2 phenotype despite 2–5 fold overexpression, whereas mutations in the guanyl kinase domain had no effect on the rescue (Hoskins *et al.*, 1996). Thus, the developmental defects that arise in the absence of CASK might be linked to the kinase function of CASK CaM-kinase domain. In non-neuronal cells, CASK-interacting adhesion molecules of the syndecan or JAM families could be substrates (Cohen *et al.*, 1998; Hsueh *et al.*, 1998; Martinez-Estrada *et al.*, 2001). These molecules share the PDZ-domain mediated CASK-association, and at least in the case of syndecan-2, serine residues in the cytoplasmic tail homologous to those of neurexins are phosphorylated *in vivo* (Itano *et al.*, 1996).

Kinase activity of CASK suggests the possibility of regulated phosphorylation of other interactors as well, such as Mint-1, liprin, Ether-a-gogo, PARKIN and CaMKII (Fallon *et al.*, 2002; Hodge *et al.*, 2006; Lu *et al.*, 2003; Marble *et al.*, 2005).

Finally, of the 518 known kinases in the human genome, 48 are predicted to be pseudokinases (Boudeau *et al.*, 2006). Each of these have one or more of the invariant motifs altered through evolution. Nine of the presumed pseudokinases, including CASK, lack a canonical DFG motif. Furthermore, this motif is altered along with other canonical motifs (HRD and/or VAIK) in 22 additional pseudokinases. Therefore, other pseudokinases, especially those with atypical DFG motifs, could be active in physiologically relevant environments; suggesting that the catalytically active kinome may be more diverse than originally envisioned.

Experimental procedures

Experimental Procedures for structural and mass-spectrometric studies can be found in the Supplementary Material.

TNP-ATP binding assay

TNP-ATP was acquired from Molecular Probes Inc. (Eugene, OR, USA). Experiments were performed in 50 mM Tris-HCl, pH 7.2, 50 mM KCl in 1 cm × 1 cm fluorescence cuvettes at 25°C using a Jobin Yvon-Spex Fluoromax-2 (Stewart *et al.*, 1998). Samples were excited at 410 nm, and emission spectra scanned from 500–600 nm. Excitation and emission slits were set at 3 and 5 nm, respectively. For TNP-ATP titration experiments, fluorescence emission at 541 nm was measured and corrected by subtracting the signal from a TNP-ATP buffer control, in which BSA replaced CASK CaM-kinase domain. For magnesium titration experiments 1 μM of TNP-ATP was mixed with 1 μM protein in a cuvette and emission was recorded at 541 nm after addition of defined quantities of Mg^{2+}.

In vitro phosphorylation assays

In the Tris-Cl buffer supplemented with 2 mM EDTA, recombinant CASK CaM-kinase domain was incubated for increasing lengths of time with 1 mM γ^{32}P-ATP (2×10^7 cpm) for 1 h at RT. For determining the K_m^{ATP} increasing concentration of ATP was added for 30 min. The protein was separated with SDS-PAGE and visualized on a phosphorimager. The

radioactivity incorporated in the band was determined for quantification. Coomassie staining was used for loading control.

GST-neurexin-1 C-tail, which comprised the entire cytoplasmic domain of neurexin-1 (AMYKYRNRDEGSYHVDESRNYISNSAQSNGAVVKEKQPSSAKSANKNKKNKDKEYYV), was bound to glutathione beads and incubated overnight with full-length CASK, in Tris-Cl buffer at 4 °C. After washing 3 times in ice-cold Tris-Cl buffer, the complexes were incubated with indicated concentrations of γ^{32}P-ATP in Tris-Cl buffer supplemented with EDTA (2 mM) or Mg (2 mM) at RT for indicated times. The proteins were eluted from the beads by thrombin cleavage, separated with SDS-PAGE and visualized on a phosphorimager. Radioactivity incorporated was calculated by correlating the beta counts in a band (measured with a Beckman-Coulter LS-6000 scintillation system) with its phosphorimager quantification (performed with Molecular Dynamics Storm scanner and Image-Quant software).

Fluorescence imaging

HEK293T cells were co-transfected with EGFP-CASK in pEGFP-C3 vector and neurexin-1β-cherry in pCAAG vector or the empty pCAAG vector using FUGENE-6 (Roche). 2 days post-transfection, the cells were washed in PBS and fixed in 4 % paraformaldehyde in PBS at RT for 20 min. Laser scanning confocal microscopy was performed to compare localization, on a Leica TCS SP-2, inverted microscope.

In vivo kinase activity assays

Primary mixed hippocampal cultures from P1 rat pups were transfected on 6 days *in vitro* (DIV) using a modified Ca^{2+}-phosphate method. Two days later, the cells were kept in 500 nM TTX and 50 μM APV overnight. Subsequently, the cells were washed and incubated in phosphate-free depletion-buffer for 30 min at 37 °C (10 mM HEPES-NaOH, pH 7.2, 150 mM NaCl, 4 mM KCl, 2 mM $MgCl_2$, 2 mM $CaCl_2$, 10 mM D-glucose, 100 μM insulin), followed by incubation in the same buffer, supplemented with 100 μCi ^{32}P-orthophosphate for 1 h. Cells were washed twice with phosphate-free buffer and lysed in ice cold solubilization buffer (10 mM Tris-Cl, pH 6.8, 150 mM NaCl, 1 % Triton-X100, 4 mM EDTA), supplemented with protease inhibitor cocktail (leupeptin, pepstatin, PMSF and aprotinin), phosphatase inhibitor cocktails-1 and 2 (Sigma). Debris was spun down (14,000 rpm for 10 min at 4 °C) and supernatant was incubated with immobilized GST-CASK PDZ-domain overnight. Complexes were washed in solubilization buffer 3 times and separated by SDS-PAGE, followed by phosphorimager scanning. β-neurexins immunoblots (pan- β-neurexins rabbit polyclonal antibody (Suppl. Fig. S12) were used as loading control. Neuronal lysates were also separated and immunoblotted for CASK with mouse monoclonal antibody (Transduction Labs).

Conditional CASK knockin-knockout mice were generated and used for primary hippocampal neuronal culture as described (Atasoy *et al.*, 2007). In brief, primary hippocampal cultures from CASK knock-in mice, containing Lox-P sites flanking the *CASK* gene, were transduced with GFP-Cre recombinase fusion protein, using a lentiviral vector system at DIV 4. Six days later (DIV 10), *in vivo* ^{32}P-phosphorylation assay was performed as described above.

HEK293T cells were co-transfected with EGFP-CASK and flag-tagged neurexin-1β. Phosphorylation and lysis were performed as above, with the exception of TTX and APV treatment. Neurexin-1β was batch precipitated on anti-flag (M-2) beads (Sigma), separated on SDS-PAGE and quantified by phosphorimager. Coomassie staining was used for visualizing total proteins loaded.

Supplementary Material

Refer to Web version on PubMed Central for supplementary material.

Acknowledgments

We thank Drs. Elizabeth Goldsmith, A. J. Robison, Mark Etherton, Gottfried Mieskes, Antony Boucard and Ralf Jauch for comments on the manuscript; members of the Südhof and Jahn laboratories for discussions; Lin Fan, Andrea Roth and Izabella Kornblum for technical support; and Reinhard Lührmann for the use of crystallography equipment. This work was supported by a grant from the NIMH (R37 MH52804-08 to TCS) and the Max-Planck-Society. MS is a Human Frontiers Long Term Fellow.

References

Abel ES, Davids BJ, Robles LD, Loflin CE, Gillin FD, Chakrabarti R. Possible roles of protein kinase A in cell motility and excystation of the early diverging eukaryote Giardia lamblia. J Biol Chem. 2001; 276:10320–10329. [PubMed: 11104758]

Adams JA. Kinetic and catalytic mechanisms of protein kinases. Chem Rev. 2001; 101:2271–2290. [PubMed: 11749373]

Atasoy D, Schoch S, Ho A, Nadasy KA, Liu X, Zhang W, Mukherjee K, Nosyreva ED, Fernandez-Chacon R, Missler M, et al. Deletion of CASK in mice is lethal and impairs synaptic function. Proc Natl Acad Sci U S A. 2007

Biederer T, Sara Y, Mozhayeva M, Atasoy D, Liu X, Kavalali ET, Sudhof TC. SynCAM, a synaptic adhesion molecule that drives synapse assembly. Science. 2002; 297:1525–1531. [PubMed: 12202822]

Biederer T, Sudhof TC. CASK and protein 4.1 support F-actin nucleation on neurexins. J Biol Chem. 2001; 276:47869–47876. [PubMed: 11604393]

Bilwes AM, Quezada CM, Croal LR, Crane BR, Simon MI. Nucleotide binding by the histidine kinase CheA. Nat Struct Biol. 2001; 8:353–360. [PubMed: 11276258]

Borg JP, Straight SW, Kaech SM, de Taddeo-Borg M, Kroon DE, Karnak D, Turner RS, Kim SK, Margolis B. Identification of an evolutionarily conserved heterotrimeric protein complex involved in protein targeting. J Biol Chem. 1998; 273:31633–31636. [PubMed: 9822620]

Boudeau J, Miranda-Saavedra D, Barton GJ, Alessi DR. Emerging roles of pseudokinases. Trends Cell Biol. 2006

Brocard JB, Rajdev S, Reynolds IJ. Glutamate-induced increases in intracellular free Mg2+ in cultured cortical neurons. Neuron. 1993; 11:751–757. [PubMed: 8104432]

Butz S, Okamoto M, Sudhof TC. A tripartite protein complex with the potential to couple synaptic vesicle exocytosis to cell adhesion in brain. Cell. 1998; 94:773–782. [PubMed: 9753324]

Cline H. Synaptogenesis: a balancing act between excitation and inhibition. Curr Biol. 2005; 15:R203–205. [PubMed: 15797012]

Cohen AR, Woods DF, Marfatia SM, Walther Z, Chishti AH, Anderson JM. Human CASK/LIN-2 binds syndecan-2 and protein 4.1 and localizes to the basolateral membrane of epithelial cells. J Cell Biol. 1998; 142:129–138. [PubMed: 9660868]

Daniels DL, Cohen AR, Anderson JM, Brunger AT. Crystal structure of the hCASK PDZ domain reveals the structural basis of class II PDZ domain target recognition. Nat Struct Biol. 1998; 5:317–325. [PubMed: 9546224]

Dimitratos SD, Stathakis DG, Nelson CA, Woods DF, Bryant PJ. The location of human CASK at Xp11.4 identifies this gene as a candidate for X-linked optic atrophy. Genomics. 1998; 51:308–309. [PubMed: 9722958]

Fallon L, Moreau F, Croft BG, Labib N, Gu WJ, Fon EA. Parkin and CASK/LIN-2 associate via a PDZ-mediated interaction and are co-localized in lipid rafts and postsynaptic densities in brain. J Biol Chem. 2002; 277:486–491. [PubMed: 11679592]

Foskett JK, White C, Cheung KH, Mak DO. Inositol trisphosphate receptor Ca2+ release channels. Physiol Rev. 2007; 87:593–658. [PubMed: 17429043]

Froyen G, Van Esch H, Bauters M, Hollanders K, Frints SG, Vermeesch JR, Devriendt K, Fryns JP, Marynen P. Detection of genomic copy number changes in patients with idiopathic mental retardation by high-resolution X-array-CGH: important role for increased gene dosage of XLMR genes. Hum Mutat. 2007

Goldberg J, Nairn AC, Kuriyan J. Structural basis for the autoinhibition of calcium/calmodulin-dependent protein kinase I. Cell. 1996; 84:875–887. [PubMed: 8601311]

Gotoh H, Kajikawa M, Kato H, Suto K. Intracellular Mg2+ surge follows Ca2+ increase during depolarization in cultured neurons. Brain Res. 1999; 828:163–168. [PubMed: 10320737]

Graf ER, Zhang X, Jin SX, Linhoff MW, Craig AM. Neurexins induce differentiation of GABA and glutamate postsynaptic specializations via neuroligins. Cell. 2004; 119:1013–1026. [PubMed: 15620359]

Hanks SK, Hunter T. Protein kinases 6. The eukaryotic protein kinase superfamily: kinase (catalytic) domain structure and classification. Faseb J. 1995; 9:576–596. [PubMed: 7768349]

Hanley RM, Means AR, Kemp BE, Shenolikar S. Mapping of calmodulin-binding domain of Ca2+/calmodulin-dependent protein kinase II from rat brain. Biochem Biophys Res Commun. 1988; 152:122–128. [PubMed: 2833884]

Hata Y, Butz S, Sudhof TC. CASK: a novel dlg/PSD95 homolog with an N-terminal calmodulin-dependent protein kinase domain identified by interaction with neurexins. J Neurosci. 1996; 16:2488–2494. [PubMed: 8786425]

Hodge JJ, Mullasseril P, Griffith LC. Activity-dependent gating of CaMKII autonomous activity by Drosophila CASK. Neuron. 2006; 51:327–337. [PubMed: 16880127]

Hoskins R, Hajnal AF, Harp SA, Kim SK. The C. elegans vulval induction gene lin-2 encodes a member of the MAGUK family of cell junction proteins. Development. 1996; 122:97–111. [PubMed: 8565857]

Hsueh YP, Wang TF, Yang FC, Sheng M. Nuclear translocation and transcription regulation by the membrane-associated guanylate kinase CASK/LIN-2. Nature. 2000; 404:298–302. [PubMed: 10749215]

Hsueh YP, Yang FC, Kharazia V, Naisbitt S, Cohen AR, Weinberg RJ, Sheng M. Direct interaction of CASK/LIN-2 and syndecan heparan sulfate proteoglycan and their overlapping distribution in neuronal synapses. J Cell Biol. 1998; 142:139–151. [PubMed: 9660869]

Huse M, Kuriyan J. The conformational plasticity of protein kinases. Cell. 2002; 109:275–282. [PubMed: 12015977]

Itano N, Oguri K, Nagayasu Y, Kusano Y, Nakanishi H, David G, Okayama M. Phosphorylation of a membrane-intercalated proteoglycan, syndecan-2, expressed in a stroma-inducing clone from a mouse Lewis lung carcinoma. Biochem J. 1996; 315(Pt 3):925–930. [PubMed: 8645178]

Jamain S, Quach H, Betancur C, Rastam M, Colineaux C, Gillberg IC, Soderstrom H, Giros B, Leboyer M, Gillberg C, et al. Mutations of the X-linked genes encoding neuroligins NLGN3 and NLGN4 are associated with autism. Nat Genet. 2003; 34:27–29. [PubMed: 12669065]

Jauch R, Cho MK, Jakel S, Netter C, Schreiter K, Aicher B, Zweckstetter M, Jackle H, Wahl MC. Mitogen-activated protein kinases interacting kinases are autoinhibited by a reprogrammed activation segment. Embo J. 2006; 25:4020–4032. [PubMed: 16917500]

Jauch R, Jakel S, Netter C, Schreiter K, Aicher B, Jackle H, Wahl MC. Crystal structures of the Mnk2 kinase domain reveal an inhibitory conformation and a zinc binding site. Structure. 2005; 13:1559–1568. [PubMed: 16216586]

Kaech SM, Whitfield CW, Kim SK. The LIN-2/LIN-7/LIN-10 complex mediates basolateral membrane localization of the C. elegans EGF receptor LET-23 in vulval epithelial cells. Cell. 1998; 94:761–771. [PubMed: 9753323]

Kargacin ME, Kargacin GJ. Predicted changes in concentrations of free and bound ATP and ADP during intracellular Ca2+ signaling. Am J Physiol. 1997; 273:C1416–1426. [PubMed: 9357788]

Kato H, Gotoh H, Kajikawa M, Suto K. Depolarization triggers intracellular magnesium surge in cultured dorsal root ganglion neurons. Brain Res. 1998; 779:329–333. [PubMed: 9473713]

Kwiatkowski AP, King MM. Mapping of the adenosine 5'-triphosphate binding site of type II calmodulin-dependent protein kinase. Biochemistry. 1987; 26:7636–7640. [PubMed: 2827758]

Leonoudakis D, Conti LR, Radeke CM, McGuire LM, Vandenberg CA. A multiprotein trafficking complex composed of SAP97, CASK, Veli, and Mint1 is associated with inward rectifier Kir2 potassium channels. J Biol Chem. 2004; 279:19051–19063. [PubMed: 14960569]

Lise MF, El-Husseini A. The neuroligin and neurexin families: from structure to function at the synapse. Cell Mol Life Sci. 2006; 63:1833–1849. [PubMed: 16794786]

Lopes C, Gassanova S, Delabar JM, Rachidi M. The CASK/Lin-2 Drosophila homologue, Camguk, could play a role in epithelial patterning and in neuronal targeting. Biochem Biophys Res Commun. 2001; 284:1004–1010. [PubMed: 11409895]

Lu CS, Hodge JJ, Mehren J, Sun XX, Griffith LC. Regulation of the Ca2+/CaM-responsive pool of CaMKII by scaffold-dependent autophosphorylation. Neuron. 2003; 40:1185–1197. [PubMed: 14687552]

Mak DO, McBride S, Foskett JK. ATP regulation of type 1 inositol 1,4,5-trisphosphate receptor channel gating by allosteric tuning of Ca(2+) activation. J Biol Chem. 1999; 274:22231–22237. [PubMed: 10428789]

Manning G, Whyte DB, Martinez R, Hunter T, Sudarsanam S. The protein kinase complement of the human genome. Science. 2002; 298:1912–1934. [PubMed: 12471243]

Marble DD, Hegle AP, Snyder ED 2nd, Dimitratos S, Bryant PJ, Wilson GF. Camguk/CASK enhances Ether-a-go-go potassium current by a phosphorylation-dependent mechanism. J Neurosci. 2005; 25:4898–4907. [PubMed: 15901771]

Martin JR, Ollo R. A new Drosophila Ca2+/calmodulin-dependent protein kinase (Caki) is localized in the central nervous system and implicated in walking speed. Embo J. 1996; 15:1865–1876. [PubMed: 8617233]

Martinez-Estrada OM, Villa A, Breviario F, Orsenigo F, Dejana E, Bazzoni G. Association of junctional adhesion molecule with calcium/calmodulin-dependent serine protein kinase (CASK/LIN-2) in human epithelial caco-2 cells. J Biol Chem. 2001; 276:9291–9296. [PubMed: 11120739]

Maximov A, Sudhof TC, Bezprozvanny I. Association of neuronal calcium channels with modular adaptor proteins. J Biol Chem. 1999; 274:24453–24456. [PubMed: 10455105]

Missler M, Zhang W, Rohlmann A, Kattenstroth G, Hammer RE, Gottmann K, Sudhof TC. Alpha-neurexins couple Ca2+ channels to synaptic vesicle exocytosis. Nature. 2003; 423:939–948. [PubMed: 12827191]

Nam CI, Chen L. Postsynaptic assembly induced by neurexin-neuroligin interaction and neurotransmitter. Proc Natl Acad Sci U S A. 2005; 102:6137–6142. [PubMed: 15837930]

Nirmala J, Brueggeman R, Maier C, Clay C, Rostoks N, Kannangara CG, von Wettstein D, Steffenson BJ, Kleinhofs A. Subcellular localization and functions of the barley stem rust resistance receptor-like serine/threonine-specific protein kinase Rpg1. Proc Natl Acad Sci U S A. 2006; 103:7518–7523. [PubMed: 16648249]

Nix SL, Chishti AH, Anderson JM, Walther Z. hCASK and hDlg associate in epithelia, and their src homology 3 and guanylate kinase domains participate in both intramolecular and intermolecular interactions. J Biol Chem. 2000; 275:41192–41200. [PubMed: 10993877]

Nolen B, Taylor S, Ghosh G. Regulation of protein kinases; controlling activity through activation segment conformation. Mol Cell. 2004; 15:661–675. [PubMed: 15350212]

Olsen O, Moore KA, Fukata M, Kazuta T, Trinidad JC, Kauer FW, Streuli M, Misawa H, Burlingame AL, Nicoll RA, et al. Neurotransmitter release regulated by a MALS-liprin-alpha presynaptic complex. J Cell Biol. 2005; 170:1127–1134. [PubMed: 16186258]

Olsen O, Moore KA, Nicoll RA, Bredt DS. Synaptic transmission regulated by a presynaptic MALS/Liprin-alpha protein complex. Curr Opin Cell Biol. 2006; 18:223–227. [PubMed: 16504495]

Rubin LJ, Brown JE. [ATP]i in Limulus photoreceptors: no correlation with responsiveness or discrete event rate. Am J Physiol. 1988; 254:C27–36. [PubMed: 2827510]

Schuh K, Uldrijan S, Gambaryan S, Roethlein N, Neyses L. Interaction of the plasma membrane Ca2+ pump 4b/CI with the Ca2+/calmodulin-dependent membrane-associated kinase CASK. J Biol Chem. 2003; 278:9778–9783. [PubMed: 12511555]

Setou M, Nakagawa T, Seog DH, Hirokawa N. Kinesin superfamily motor protein KIF17 and mLin-10 in NMDA receptor-containing vesicle transport. Science. 2000; 288:1796–1802. [PubMed: 10846156]

Smith MK, Colbran RJ, Brickey DA, Soderling TR. Functional determinants in the autoinhibitory domain of calcium/calmodulin-dependent protein kinase II. Role of His282 and multiple basic residues. J Biol Chem. 1992; 267:1761–1768. [PubMed: 1309796]

Stewart RC, VanBruggen R, Ellefson DD, Wolfe AJ. TNP-ATP and TNP-ADP as probes of the nucleotide binding site of CheA, the histidine protein kinase in the chemotaxis signal transduction pathway of Escherichia coli. Biochemistry. 1998; 37:12269–12279. [PubMed: 9724541]

Szatmari P, Paterson AD, Zwaigenbaum L, Roberts W, Brian J, Liu XQ, Vincent JB, Skaug JL, Thompson AP, Senman L, et al. Mapping autism risk loci using genetic linkage and chromosomal rearrangements. Nat Genet. 2007; 39:319–328. [PubMed: 17322880]

Tabuchi K, Biederer T, Butz S, Sudhof TC. CASK participates in alternative tripartite complexes in which Mint 1 competes for binding with caskin 1, a novel CASK-binding protein. J Neurosci. 2002; 22:4264–4273. [PubMed: 12040031]

Taylor JS, Vigneron DB, Murphy-Boesch J, Nelson SJ, Kessler HB, Coia L, Curran W, Brown TR. Free magnesium levels in normal human brain and brain tumors: 31P chemical-shift imaging measurements at 1.5 T. Proc Natl Acad Sci U S A. 1991; 88:6810–6814. [PubMed: 1650484]

Taylor SS, Yang J, Wu J, Haste NM, Radzio-Andzelm E, Anand G. PKA: a portrait of protein kinase dynamics. Biochim Biophys Acta. 2004; 1697:259–269. [PubMed: 15023366]

Tereshko V, Teplova M, Brunzelle J, Watterson DM, Egli M. Crystal structures of the catalytic domain of human protein kinase associated with apoptosis and tumor suppression. Nat Struct Biol. 2001; 8:899–907. [PubMed: 11573098]

Ushkaryov YA, Petrenko AG, Geppert M, Sudhof TC. Neurexins: synaptic cell surface proteins related to the alpha-latrotoxin receptor and laminin. Science. 1992; 257:50–56. [PubMed: 1621094]

Waas WF, Rainey MA, Szafranska AE, Cox K, Dalby KN. A kinetic approach towards understanding substrate interactions and the catalytic mechanism of the serine/threonine protein kinase ERK2: identifying a potential regulatory role for divalent magnesium. Biochim Biophys Acta. 2004; 1697:81–87. [PubMed: 15023352]

Warmuth M, Kim S, Gu XJ, Xia G, Adrian F. Ba/F3 cells and their use in kinase drug discovery. Curr Opin Oncol. 2007; 19:55–60. [PubMed: 17133113]

Yamagata M, Sanes JR, Weiner JA. Synaptic adhesion molecules. Curr Opin Cell Biol. 2003; 15:621–632. [PubMed: 14519398]

Zordan MA, Massironi M, Ducato MG, Te Kronnie G, Costa R, Reggiani C, Chagneau C, Martin JR, Megighian A. Drosophila CAKI/CMG protein, a homolog of human CASK, is essential for regulation of neurotransmitter vesicle release. J Neurophysiol. 2005; 94:1074–1083. [PubMed: 15872064]

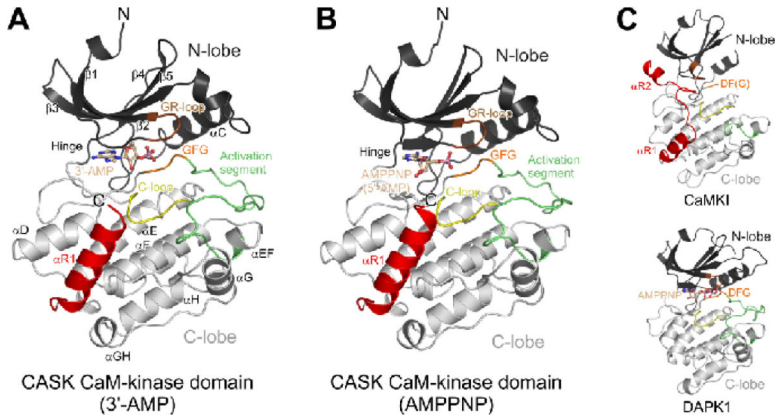

Fig. 1. Structure of the CASK CaM-kinase domain and Comparison with other CaM-kinases

A, **B**. Ribbon diagrams depicting the overall fold of the CASK CaM-kinase domain in complex with 3'-AMP (orthorhombic form, **A**; see Suppl. Fig. S3 for the triclinic form) or the 5'-AMP portion of AMPPNP (triclinic form, **B**).

C, **D**. Ribbon diagrams of rat CaMKI (Goldberg *et al.,* 1996) (PDB ID 1A06) (**C**), and DAPK1 in complex with Mn^{2+}-AMPPNP (Tereshko *et al.,* 2001) (PDB ID 1IG1) (**D**).

All structures are shown in the same orientation with the N-terminal lobes (dark gray) at the top and the C-terminal lobes (light gray) at the bottom. Specific structural elements are color-coded: Portion of the glycine-rich loop (GR-loop) – brown; catalytic loop (C-loop) – yellow; D/GFG of the magnesium binding loop – orange (the third residue is disordered in the CamKI structure); activation segment – green; C-terminal Ca^{2+}/CaM-binding segment (CaM-segment) – red. The region between the helices αR1 and αR2 of the regulatory segment is placed in the ATP-binding cleft between N- and C-terminal lobe in CaMKI, and interacts with the tip of the GR-loop. The same element is partially disordered and does not interact with the ATP binding pocket in the CASK CaM-kinase domain. Bound nucleotides in (**A**) (3'-AMP), (**B**) (5'-AMP portion of AMPPNP) and (**D**) (AMPPNP) are shown in ball-and-sticks.

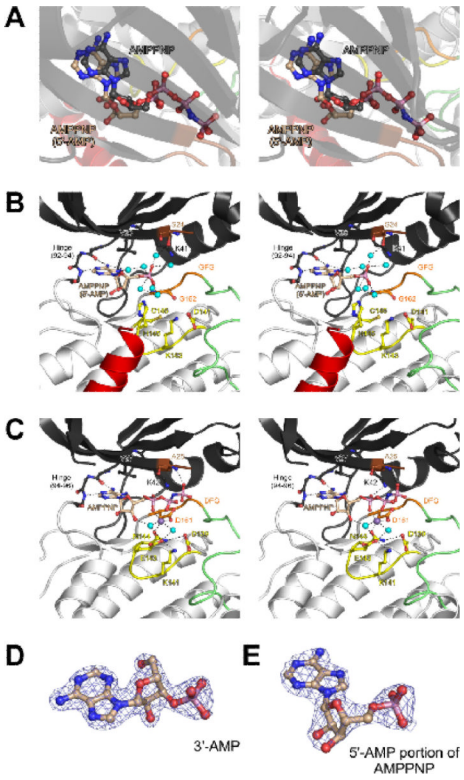

Fig. 2. Architecture of the CASK CaM-kinase domain nucleotide binding pocket

A. Stereo views comparing the positions of 5'-AMP and AMPPNP in the context of CaM-kinase domain nucleotide binding clefts, after global superpositioning of the DAPK1-AMPPNP co-crystal structure onto the CASK CaM-kinase domain-5'-AMP co-crystal structure; carbon of AMPPNP – gray.

B, **C**. Stereo plots of the nucleotide binding pockets of the CASK (**B**, in a complex with 5'-AMP (triclinic form)) and the DAPK1 CaM-kinase domains (**C**, in a complex with AMPPNP (pdb ID 1IG1)). Strand β1 and part of the Gly-rich loops have been cut away for an unobstructed view. Portions of the Gly-rich loops (carbon – brown), the catalytic-loops (carbon – yellow), the magnesium binding loops (carbon – orange; GFG and DFG, respectively) and the nucleotides (carbon – beige) are shown (ball-and-stick). Water molecules are displayed as cyan spheres. A Mn^{2+} ion in the DAPK1-AMPPNP co-crystal structure is shown as a purple sphere. Other protein elements and atoms are color-coded as in Fig. 1. Hydrogen bonds and salt bridges are shown as dashed lines. The hinge regions (only backbone atoms are shown; residue numbers are indicated) connecting the N- and C-terminal lobes and critical residues discussed in the text are labeled.

D, **E**. Electron density around the bound nucleotides. $2F_o$-F_c electron density maps contoured at the 1**σ** level around the nucleotides bound to CASK CaM-kinase domain are shown for the 3'-AMP of the orthorhombic crystal form (**D**), and the 5'-AMP portion of AMPPNP in the soaked triclinic crystal form (**E**). Atoms of the nucleotides are color-coded by atom type as before.

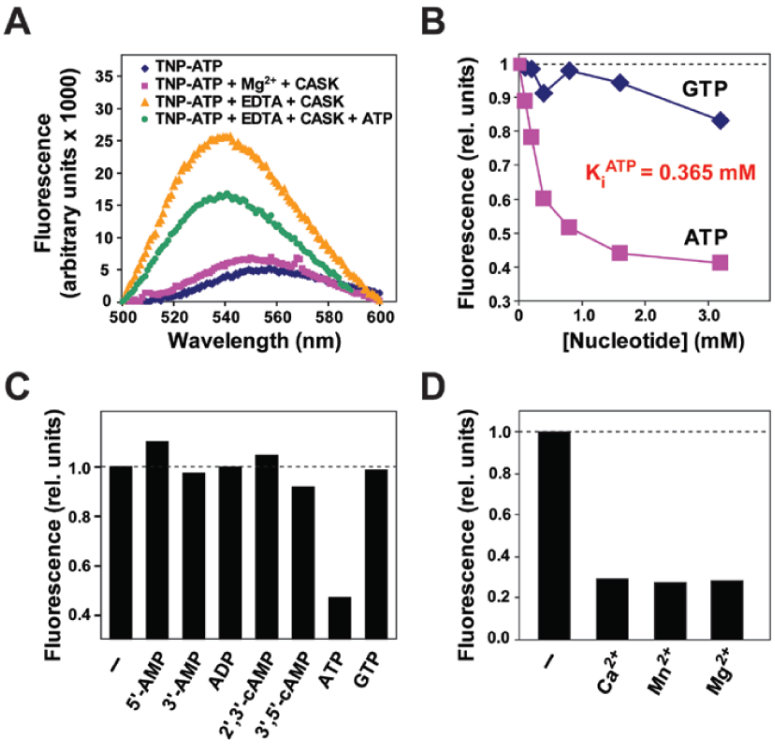

Fig. 3. Nucleotide binding by the CASK CaM-kinase domain: Inhibition by divalent ions

A. Fluorescence emission spectra (excitation = 410 nM) of TNP-ATP (1 μM) in Tris-Cl buffer containing 2 mM $MgCl_2$ in the absence of the CASK CaM-kinase domain (blue), or after addition of CASK CaM-kinase domain (1 μM; red), and after subsequent addition of EDTA (4 mM, to remove the Mg^{2+}; yellow trace), and of Na^{+}-ATP (500 μM; green) to the same cuvette.

B. Titration of the TNP-ATP (1 μM) fluorescence as a function of the GTP- and ATP-concentration in two parallel cuvettes containing CASK CaM-kinase domain (1 μM) in Tris-Cl buffer supplemented with 4 mM EDTA (excitation = 410 nM; emission = 540 nM). Data shown represent fluorescence units after subtraction of the TNP-ATP fluorescence background, normalized to the initial reading (rel. units).

C. Inhibition of the TNP-ATP interaction with the CASK CaM-kinase domain by adenine nucleotides. The fluorescence (excitation = 410 nM; emission = 540 nM) of the CASK CaM-kinase domain/TNP-ATP complex (1 μM each) was measured in EDTA (4 mM) before and after addition of the indicated nucleotides (500 μM each). Fluorescence units were normalized to the respective initial readings (rel. units), following background subtraction.

D. Inhibition of TNP-ATP binding to the CASK CaM-kinase domain by divalent ions. The fluorescence (excitation = 410 nM; emission = 540 nM) of the CASK CaM-kinase domain/TNPATP complex (1 μM each) was measured in Tris-Cl buffer supplemented with EDTA (4 mM) or 2 mM of the indicated divalent cations. The data represent normalized fluorescent units (rel. units) with background subtraction. For Mg^{2+}-dependent inhibition of radioactive ATP-binding, see Suppl. Fig. S6A.

Representative data from three independent experiments are shown in each panel.

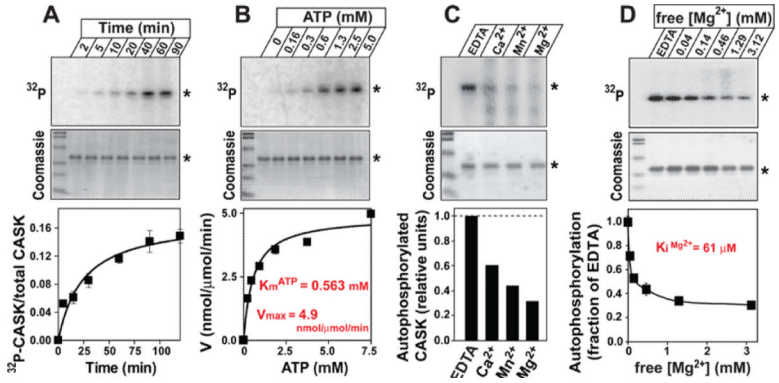

Fig. 4. Autophosphorylation of the CASK CaM-kinase domain

All experiments were performed at room temperature with purified CASK CaM-kinase domain (1 μM) incubated with γ^{32}P-ATP (specific activity: 2×10^7 cpm) in Tris-Cl buffer containing 2 mM EDTA or the indicated additions. For each experiment, the upper panels depict representative autoradiograms and Coomassie stains of SDS-gels (asterisk indicates the CASK CaM-kinase domain), and the lower panels represent summary graphs of the autophosphorylation of CASK CaM-kinase domain as measured by phosphorimager. Radioactivity incorporated was calculated by relating the β-counts in a band to its phosphorimager quantification and protein content. Data shown are means ± SEMs (n=3).

A. Time course of CASK CaM-kinase domain autophosphorylation in the presence of 1mM ATP.

B. Measurement of CASK CaM-kinase domain autophosphorylation as a function of the ATP concentration for 30 min. Michaelis constant (K_m^{ATP}) and V_{max} were calculated using Graph-Pad Prism software.

C. Decrease of CASK CaM-kinase domain autophosphorylation by divalent cations. Autophosphorylation reactions in 1mM ATP were carried out for 30 min, in the absence of (supplemented with 2 mM EDTA), or after adding 4 mM of the indicated divalent cation.

D. Effect of Mg^{2+}-titration on CASK CaM-kinase domain autophosphorylation. Reactions were carried out in buffer supplemented with either EDTA (2 mM), or the indicated amount of free-Mg^{2+} (total Mg^{2+} required was calculated with open source software WEBMAXC).

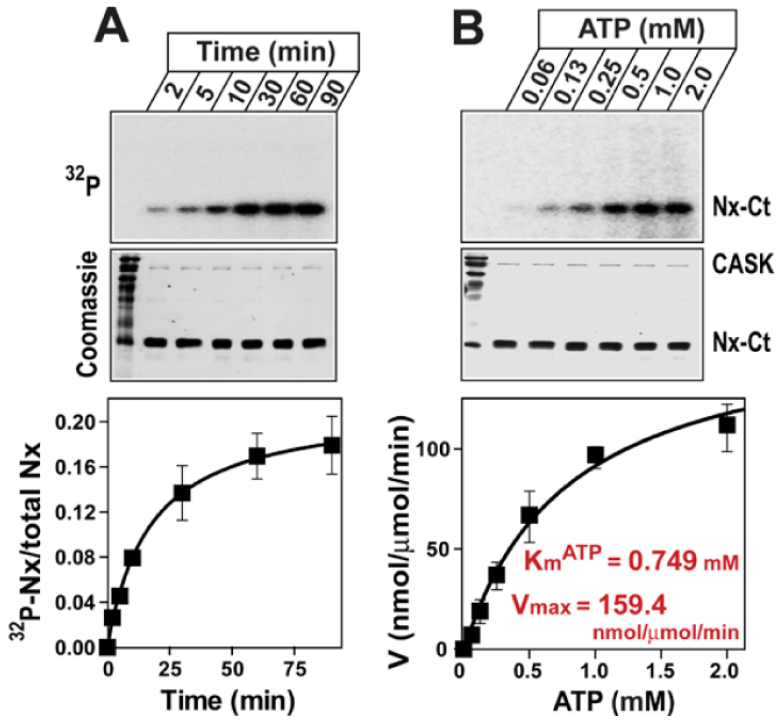

Fig. 5. Full-length CASK phosphorylates the cytoplasmic tail of neurexin-1

A. CASK-mediated phosphorylation of the cytoplasmic tail of neurexin-1 as a function of time. Full-length CASK was bound at 4 °C to the GST-neurexin-1 cytoplasmic tail (Nx-Ct) immobilized on glutathione beads, in Tris-Cl buffer containing 2 mM EDTA. The complex was washed and then incubated with γ^{32}P-ATP (2×10^7 cpm; 500 μM) at room temperature for the indicated time periods. The proteins were eluted from the beads by thrombin cleavage, separated by SDS-PAGE, and visualized on a phosphorimager. Radioactivity incorporated was calculated by relating the β-counts in a band to its phosphorimager quantification and protein content. Data shown are means ± SEM (n=3). Mass spectroscopy revealed that the peptides comprising residues 422 to 433 of neurexin-1 (QPSSAKSANKNK) were phosphorylated at one or two serine residues (data not shown). Note that the phosphorylation of the neurexin-1 cytoplasmic tail by the isolated CASK CaM-kinase domain (lacking the PDZ-domain of CASK) is inefficient (Suppl. Fig. S7A).

B. ATP-concentration dependent phosphorylation of the cytoplasmic tail of neurexin-1. The complex of full-length CASK with the GST-neurexin-1 C-terminal tail protein was incubated in Tris-Cl buffer containing 2 mM EDTA and increasing amounts of γ^{32}P-ATP for 30 min at room temperature. The Michaelis constant (K_m^{ATP}) and V_{max} were calculated as described above (means ± SEMs, n=3).

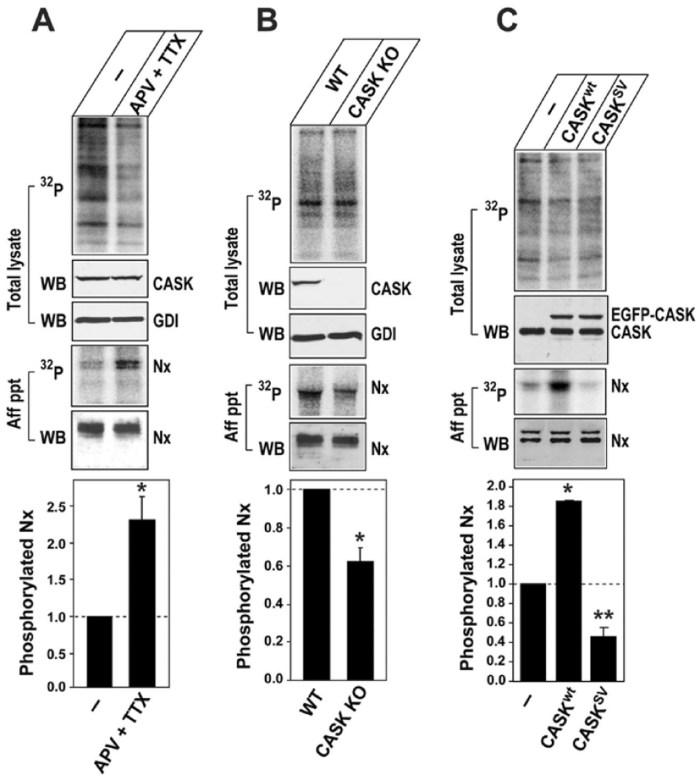

Fig. 6. CASK phosphorylates endogenous neurexins in cultured neurons

A. Neurexin phosphorylation in neurons is reduced by synaptic activity, in contrast with total ^{32}P incorporation. Rat hippocampal cultures (DIV 14) were treated with 50 μM APV and 500 nM TTX (APV + TTX) or vehicle (−) overnight. Subsequently, *in vivo* ^{32}P-phosphorylation assay was performed in the presence of TTX and APV or the vehicle. Total lysate was separated on SDS-PAGE and quantified from phosphorimager scans. Compared to active neurons, total ^{32}P incorporated was significantly reduced in silenced neurons (≈ 58 ± 1.8 %). Neurexins were affinity-purified (Aff ppt) on immobilized CASK PDZ-domain, and the proteins were separated on SDS-PAGE followed by transfer onto a nitrocellulose membrane. A phosphorimager scan was used to visualize the phosphorylated β-neurexins (^{32}P, Nx), followed by immunoblotting (WB) for β-neurexins (Nx). Lysates were also probed for CASK expression and GDI as a control for total cellular protein. Phosphorylated total proteins under each condition were also detected by phosphorimager scanning (see Suppl. Fig. S9), with a notable reduction in the total ^{32}P incorporated by inactivated neurons. The bar graph depicts β-neurexin phosphorylation levels in the active and silenced neurons. Data are represented as means ± SEM, n = 6; asterisk, P = 0.0128.

B. Neurexin phosphorylation is reduced in CASK knockout neurons. Mouse hippocampal cultures from wild type and CASK conditional knockout mice were transduced with lentiviral vector expressing Cre recombinase-GFP fusion protein at DIV 4. Six days later (DIV 10), *in vivo* ^{32}P-phosphorylation assay was performed in the presence of TTX and APV. Total lysate was separated on SDS-PAGE and visualized with phosphorimager scanning (top panel). Neurexins were affinity-purified (Aff ppt) on immobilized CASK PDZ-domain, and the proteins were separated on SDS-PAGE, followed by transfer onto a nitrocellulose membrane. Phosphorylated β-neurexins were visualized with phosphorimager scanning (^{32}P, Nx), followed by immunoblotting (WB) for β-neurexins (Nx). Lysates were also probed for CASK and GDI. Bar graph depicts β-neurexin phosphorylation levels in the

wild type (WT)_and CASK knockout (KO) neurons. Data are represented as means ± SEM, n = 6; asterisk, P = 0.000308.

C. CASK efficiently phosphorylates endogenous neurexin in neurons. Rat hippocampal cultures (DIV 6) were transfected at high efficiency with empty vector (−), wild-type EGFP-CASK fusion protein ($CASK^{wt}$), or SV-mutant EGFP-CASK fusion protein ($CASK^{SV}$), using a modified calcium-phosphate method. 72 h later, an *in vivo* phosphorylation assay was performed with $^{32}P_i$ in the presence of TTX and APV. Total lysate was separated on SDS-PAGE and visualized with phosphorimager scanning (top panel). Neurexins were affinity-purified (Aff ppt) on immobilized CASK PDZ-domain, and proteins were separated on SDS-PAGE and transferred onto a nitrocellulose membrane. A phosphorimager scan was used to visualize the phosphorylated β-neurexins (^{32}P, Nx), followed by immunoblotting (WB) for β-neurexins (Nx); the upper band correlates with the radioactive signal. Lysates were also probed for CASK (bottom panel); lower bands represent endogenous CASK and upper bands EGFP-CASK. Bar graph depicts β-neurexin phosphorylation levels in CASK transfected neurons as compared to the untransfected neurons. Data are represented as means ± SD, n = 3; single asterisk, $P = 2.9 \times 10^{-5}$; double asterisk, P = 0.0016.

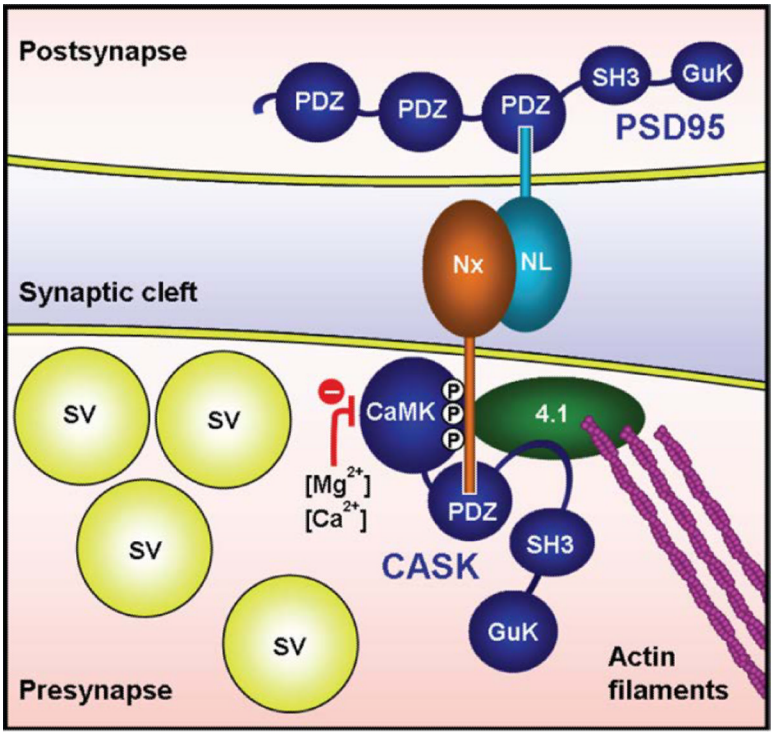

Fig. 7. Model of neurexin phosphorylation by CASK

Neurexin (Nx) and neuroligin (NL) are thought to interact extracellularly with each other across the synapse, and associate intracellularly with the MAGUKs CASK and PSD-95, respectively. The model proposes that CASK is recruited to the cytosolic C-tail of neurexin via the CASK PDZ-domain, and subsequently phosphorylates the neurexin C-terminal tail. Protein 4.1, which binds the C-tail of neurexin as well as CASK, nucleates actin filaments, modulating the pre-synaptic cytoskeleton. On the presynaptic side, CASK is shown in dark blue (CaM-kinase domain (CaMK), PDZ domain (PDZ), SH3 domain (SH3), guanyl kinase domain (GuK)), neurexin is in orange (Nx), protein 4.1 is in green (4.1), actin filaments are in pink, and synaptic vesicles are in yellow (SV). On the postsynaptic side, PSD95 is shown in dark blue and neuroligin is in light blue (NL). Red indicator depicts the inhibition of CASK CaM-kinase activity due to increase in cytosolic divalent cations.